Optimization of the Supply Voltage System in Interleaved Converters Using Intercell Transformers

François Forest, Thierry Meynard, E. Labouré, Valentin Costan, Emmanuel Sarraute, Alain Cunière, Thierry Martiré

Optimization of the Supply Voltage System in Interleaved Converters Using Intercell Transformers

François Forest, Thierry A. Meynard, Eric Labouré, Valentin Costan, Emmanuel Sarraute, Alain Cunière, and Thierry Martiré

***Abstract*—Interleaved power converters are now used in many different conversion systems involving various topologies (series or parallel) and related to different fields or loads. This paper deals with interleaved parallel commutation cells using coupling transformers with a possibly high number of cells. The first part of the paper is a reminder of the basics of magnetic couplers addressing monolithic as well as distributed implementations.**

The limits associated with the conventional supply of such couplers (supply voltages forming a direct polyphase system) are described. In the second part of the paper, an optimized voltage supply improving the performances of the system is introduced. Experimental results obtained on a seven-cells test bench validate the approach.

***Index Terms*—Power converters, uninterruptible power supply (UPS) voltage regulator module (VRM).**

I. Introduction

INTERLEAVED converters with filtered output voltage are widely employed in various applications including voltage regulator module (VRM) (a few V, 10–100 A, 100 kHz–1 MHz) and high power uninterruptible power supplies (UPS) (a few 100 V to 1000 V, few 100 A, 10–20 kHz). Their well-known advantage is an increase of the apparent frequency of the voltage applied across the filters; associating k identical commutation cells fed by interleaved control signals (equal duty cycles, phase-shifts $= 360^\circ/k$), the apparent frequency for the filters is k times the switching frequency. In addition, an improvement of the dynamic behavior can be obtained by interleaved converters [6].

Two mains solutions can be applied to interconnect interleaved commutation cells, by means of either uncoupled or coupled inductors (addition of the cell currents) on the one hand, and by means of transformers (addition of the cell voltages), on the other hand. One of the conclusions of this paper is that transformer-based solutions must be preferred for converters with a high number of cells ($k > 4$).

In a first part, the principle of cell-coupling by transformers is recalled and the two ways of design, separate transformers or a single monolithic transformer, are presented. The properties and limitations in the case of supply by a regular voltage system are described.

In the second part, an original mode of supply, using a particular permutation of the k voltages provided by the converter cells is proposed. It leads to a large reduction of the flux in some parts of the transformers, especially for high value of k. At last, a comparison between the solutions using uncoupled inductors and those using transformers with the permutated supply is conducted, showing the great interest of the proposed solution.

F. Forest, V. Costan, and T. Martiré are with the Laboratoire d'Electrotechnique de Montpellier (LEM), Université de Montpellier II, Montpellier 34095, France (e-mail address: forest@univ-montp2.fr).

T. A. Meynard and E. Sarraute are with the Laboratoire d'Electrotechnique et d'Electronique Industrielle (LEEI), Unité Mixte de Recherche INPT-ENSEEIHT/CNRS, Toulouse 31071, France.

E. Labouré and A. Cunière are with the SATIE/ENS de Cachan, Cachan 94235, France.

II. Interleaved Parallel Converters and Magnetic Devices

The two examples of Fig. 1 (VRM and UPS) illustrate the most widespread solutions that consist of association of k cells, each of them including its own inductor operating at the switching frequency F of the cell [9].

An improvement proposed in [4] is obtained by association of two coupled cells but the magnetic device stays an inductor; in particular, it requires air gap and experiences eddy currents.

The other solution is based on the introduction of coupling transformers (or intercell transformers) [1], [3], [5]–[8] that are built by association of elementary transformers (separate transformers) or realized on a monolithic magnetic core (monolithic transformer).

A theoretical study, principally dealing with associations of separate transformers is proposed in [1]. Fig. 2 shows an example of the association of k elementary transformers referred to as "cyclic cascade configuration."

The general property of the intercell transformers is to realize the average of the k voltages provided by the converter cells

$$v_o = \frac{\sum_{p=1}^{k} v_p}{k}.$$

It is well known that in steady state the average value of the output voltage v_o is equal to the average value of any of the k voltages $v_1, \ldots, v_k$ (all the average values of the supply voltages must be identical) and presents a reduced THD (cancellation of all harmonics except those multiple of).

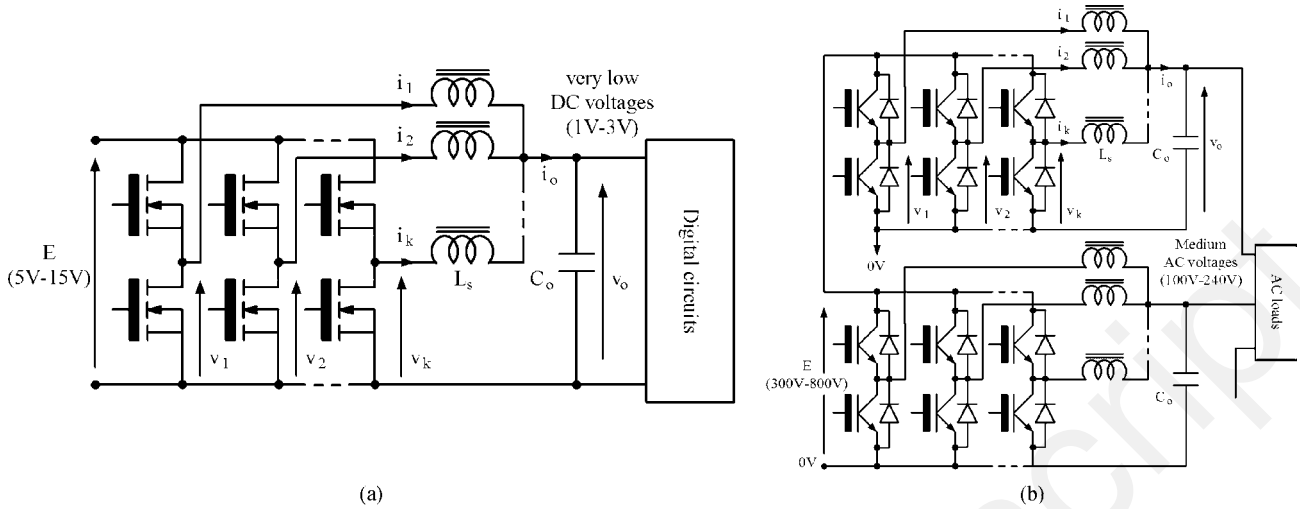

Fig. 1. Example of interleaved converters with uncoupled inductors: (a) VRM modules and (b) UPS inverter.

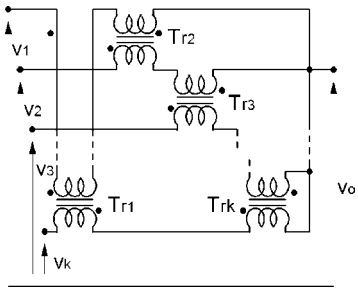

Fig. 2. Example of transformers association.

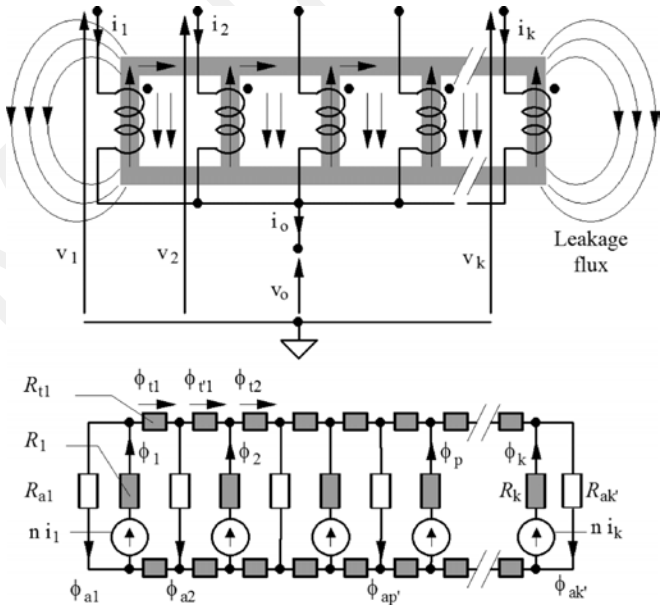

Fig. 3. Basic topology of the monolithic intercell transformer.

III. Interleaving With Intercell Transformers

A. Principle

To understand the operating principle of intercell transformers, a good introduction is the analysis of a monolithic transformer with k columns on which are placed k identical windings with n turns, as shown in Fig. 3.

The leakage flux lines circulating between the two horizontal parts of the core are schematically represented. To this basic scheme can be associated the reluctance network of the same figure. $R_1, \dots R_k$ are the reluctances of the vertical magnetic branches (called in the next main branches) where circulate the main fluxes ϕ_p. $R_{a1}, \dots, R_{a2}$ are the reluctances of the leakage zones where circulate the leakage fluxes ϕ_{ap}. At last, $R_{t1}, \dots$ are the reluctances of the horizontal magnetic branches (called in the next transversal branches) where circulate the transversal fluxes ϕ_{tp}. The windings are wound around the main branches.

A special feature of this magnetic coupler is that all the windings have one terminal connected to a voltage source (square voltages $v_1, \dots, v_k$), and the other connected to a common point; the average potential of this common point (V_o) is equal to the average of the potentials $V_1, \dots, V_k$. As a consequence, if the ac component of v_o and the winding resistances are neglected the ac voltage across winding p only depends on voltage v_p and the ac flux in winding p can be directly determined by integration of v_p.

On the other hand, the dc voltage across winding p is the average of the difference between voltage v_p and v_o, which shows that the dc flux created by a winding p is related to the voltage unbalance and depends on the full supply voltage. As a consequence, to determine how much dc flux is generated in a winding, the reluctance model showing the magnetic coupling between all the windings is needed.

The different variables are described as

$$v_p - v_o = \tilde{v}_p - \tilde{v}_o + V_p - V_o$$
$$i_p = \tilde{i}_p + I_p \text{ and } \phi_p = \tilde{\phi}_p + \Phi_p$$

with $\tilde{x}$ alternative part and X continuous part.

The basic relation available in any case is

$$v_p - v_o = r i_p + n\frac{d\phi_p}{dt} = r i_p + n\frac{d\tilde{\phi}_p}{dt} \qquad (1)$$

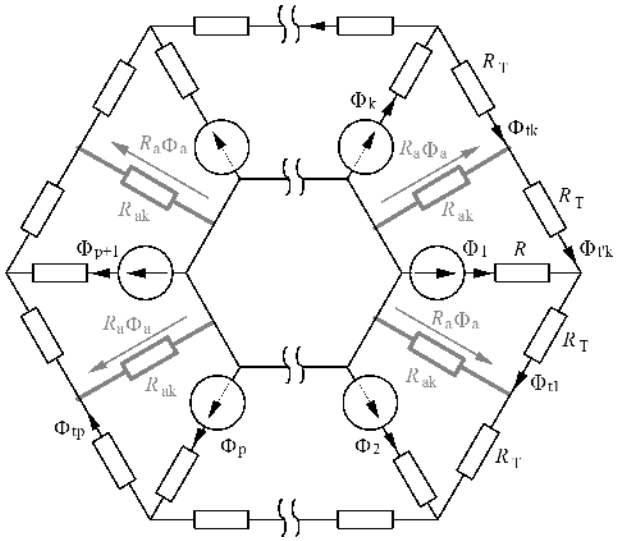

Fig. 4. Symmetrical scheme of the monolithic intercell transformer.

where r is the winding resistor.

1) Alternating Mode: In alternating mode, it is supposed that

a) I_p, nI_p and Φ_p are null;

b) the term $r\tilde{i}_p$ is negligible compared with $\tilde{v}_p - \tilde{v}_o$.

In these conditions, each main alternating flux is imposed by the alternating voltage applied to the corresponding winding [see (1)]. First, an important relation can be established between the main flux and the leakage flux. The contribution of one main flux to the total leakage flux can be obtained by considering the reluctance scheme of Fig. 3 with all other main branches opened.

So, the contribution of the branch p is such that

$$\sum_{p'=1}^{k'} \tilde{\phi}_{ap'}^{p} = \tilde{\phi}_p$$

where $\tilde{\phi}_{a,p'}^{p}$ is the flux generated in the air branch p' by $\tilde{\phi}_p$.

In this partial configuration, the magnetic potential across the transversal reluctances R_T can be considered as negligible compared to the difference of magnetic potential across the leakage reluctances R'_{ap}, because R_T is negligible compared with R'_{ap} (ratio > 1000 in practice). So, the distribution of the flux induced by one winding in the different air branches is quite independent of the reluctances RT. The distribution of the air reluctances ($R_{a1} \ldots, R_{ak'}$) and the geometry of the magnetic core are enough to determine the complete flux distribution.

This assumption can be expressed by the following simplification:

$$R_{a1}\tilde{\phi}_{a1} \cong \ldots . \cong R_{ak'}\tilde{\phi}_{ak'} \cong R_a\tilde{\phi}_a \tag{2}$$

$$\text{where } \tilde{\phi}_a = \sum_{p'=1}^{k'} \tilde{\phi}_{ap'} = \sum_{p'=1}^{k'} \tilde{\phi}_{ap'}^{1} + \cdots\cdots + \sum_{p'=1}^{k'} \tilde{\phi}_{ap'}^{k}$$

$$= \sum_{p=1}^{k} \tilde{\phi}_p \text{ and} s \sum_{p'=1}^{k'} \frac{1}{R_{ap'}} = \frac{1}{R_a}. \tag{3}$$

To simplify the next development, symmetrical topologies will be now considerate. The polygonal reluctance scheme of Fig. 4 can be used for any symmetrical topology (easy to build symmetrical topologies are discussed in Section III-B).

The reluctances in all the main branches are identical, as well the transversal reluctances, on the one hand, as well as the air reluctances, on the other hand. In this scheme, the assumption of (2) is still valid, so all the air branches see a magnetic potential equal to $R_a.\phi_a$.

Core and leakage inductors are defined as

$$L = \frac{n^2}{R'} \text{ and } L_a = \frac{n^2}{R_a}, \text{with}$$

$$R' = R + \frac{R_T}{2}, R_a = \frac{R_{ak}}{k} \text{ and } R_a \gg R'.$$

Voltage Equations:

$$\tilde{v}'_1 = \tilde{v}_1 - \tilde{v}_o = n\frac{d\tilde{\phi}_1}{dt}$$

$$\tilde{v}'_2 = \tilde{v}_2 - \tilde{v}_o = n\frac{d\tilde{\phi}_2}{dt}$$

$$\vdots$$

$$\tilde{v}'_k = \tilde{v}_k - \tilde{v}_o = n\frac{d\tilde{\phi}_k}{dt}$$

$$\sum_{p=1}^{k} \tilde{v}_p - k\tilde{v}_o = n\frac{d\tilde{\phi}_a}{dt}$$

$$\tilde{v}_o = \frac{\sum_{p=1}^{k} \tilde{v}_p}{k} - \frac{n}{k}\frac{d\tilde{\phi}_a}{dt}. \tag{4}$$

Current Equations:

$$n\tilde{i}_1 - R'\tilde{\phi}_1 = R_a\tilde{\phi}_a$$

$$n\tilde{i}_2 - R'\tilde{\phi}_2 = R_a\tilde{\phi}_a$$

$$\vdots$$

$$n\tilde{i}_k - R'\tilde{\phi}_k = R_a\tilde{\phi}_a$$

$$n\sum_{p=1}^{k} \tilde{i}_p - R'\sum_{p=1}^{k} \tilde{\phi}_p = kR_a\tilde{\phi}_a$$

$$n\tilde{i}_o = (kR_a + R')\tilde{\phi}_a. \tag{5}$$

By neglecting R' with regard to kR_a, the (5) can be simplified as

$$n\tilde{i}_o = kR_a\tilde{\phi}_a. \tag{6}$$

From (4) and (6)

$$\tilde{v}_o = \frac{\sum_{p=1}^{k} \tilde{v}_p}{k} - \frac{L_a}{k^2}\frac{d\tilde{i}_o}{dt}. \tag{7}$$

From the current equations, it can be deduced

$$\frac{n^2}{R'}\frac{d\tilde{i}_p}{dt} - n\frac{d\tilde{\phi}_p}{dt} = n\frac{R_a}{R'}\frac{d\tilde{\phi}_a}{dt} = \frac{n^2}{kR'}\frac{d\tilde{i}_o}{dt}$$

then

$$\frac{d\tilde{i}_p}{dt} = \frac{(\tilde{v}_p - \tilde{v}_o)}{L} + \frac{1}{k}\frac{d\tilde{i}_o}{dt} = \frac{d\tilde{i}_{mp}}{dt} + \frac{1}{k}\frac{d\tilde{i}_o}{dt}.$$

Finally

$$\tilde{i}_p = \tilde{i}_{mp} + \frac{\tilde{i}_o}{k} \tag{8}$$

with $L(d\tilde{i}_{mp}/dt) = \tilde{v}_p - \tilde{v}_o$.

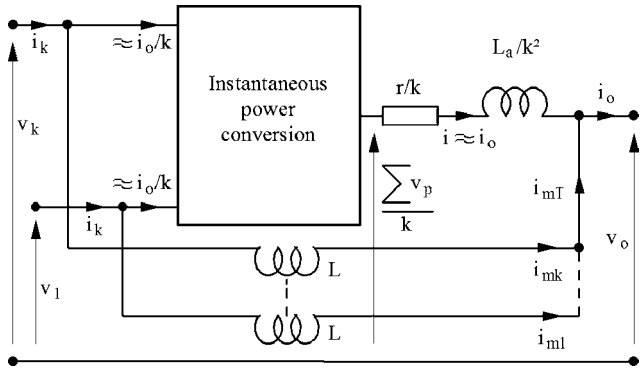

Fig. 5. Approximate model of the monolithic intercell transformer.

2) Continuous Mode: In continuous mode, the equations become

$$V_1 - V_o = rI_1 \qquad nI_1 - R'\Phi_1 = R_a\Phi_a$$
$$V_2 - V_o = rI_2 \qquad nI_2 - R'\Phi_2 = R_a\Phi_a$$

that leads to

$$V_o = \frac{\sum_{p=1}^{k} V_p}{k} - \frac{r}{k}I_o \tag{9}$$
$$nI_o = kR_a\Phi_a. \tag{10}$$

These equations show that the balancing of the average currents in the phases depends of the balancing of the average voltages across the winding and of the series resistances values.

If the average currents are unbalanced and known, the reluctance model allows calculating the dc fluxes in each branch. A small difference of current in two windings gives different magneto motive sources connected through small reluctances resulting in a possibly high dc flux.

Practically, the respect of current balancing is critical, in order to avoid the saturation of cores, and can need a passive or active balancing mechanism [2]. If the average voltage and series resistances are identical, the current in each winding is I_o/k. By supposing verified the assumption of the current balancing, the total average flux is imposed by the average value of total output current I_o, with the relation

$$\Phi_a = \frac{L_a}{nk}I_o. \tag{11}$$

From (7)–(9), an approximate model of the intercell monolithic transformer can be derived (Fig. 5). The sum of magnetizing currents i_{mT} is supposed negligible compared with the output current i_o. This condition is easily verified because i_{mT} is the sum of k interleaved magnetizing currents and its value is limited by the high value of L.

This model emphasizes the main characteristics of the intercell transformer, namely the summation of voltages and the presence of an output inductor L_a/k^2, associated to the leakage flux.

In the following, according to the assumption of high value for k, it will be considered that the output inductor value is sufficient to limit the output current ripple. So, the intercell transformer can be directly connected to an output capacitor and replaces the k inductors used in the classical solutions.

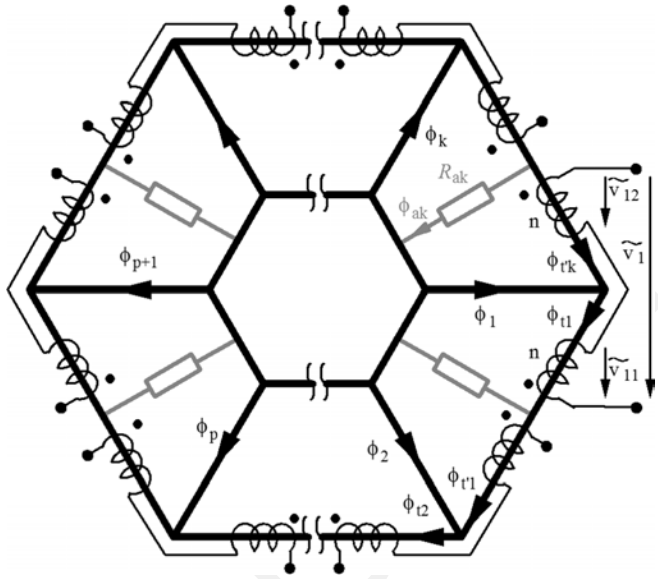

Fig. 6. Symmetrical topology with divided windings.

B. Monolithic Versus Separate Intercell Transformers

In the present section, the symmetry of the intercell transformer is supposed realized. As this section and the following only concern the flux repartition, the core reluctances are not represented in the schemes.

A topological variant of the intercell transformer described above (winding wound around the main branches) is shown in Fig. 6. It is possible to separate the windings in two parts and to distribute them on the two adjacent transversal branches. Indeed, this new configuration is described by

$$\tilde{v}_{11} + \tilde{v}_{12} = \tilde{v}_1 = n\frac{d\tilde{\phi}_{t1}}{dt} - n\frac{d\tilde{\phi}_{t'k}}{dt} = n\frac{d\tilde{\phi}_1}{dt}.$$

So, the alternative flux repartition is identical to the previous one but the configuration of the windings in a window, with opposite currents in the two half-winding, is similar to a voltage transformer configuration, and favorable to the limitation of eddy currents losses.

This particular monolithic transformer can be separated in k identical two-windings transformers (Fig. 7) and then appears the "Cyclic cascade" association of Fig. 2. This approach demonstrates the direct analogy that exists between the monolithic transformer and the associations of separated transformers as those described in [1].

If the electrical behavior of the transformers association is similar, the separation induces a significant modification. The flux circulating in a transformer is not the main flux circulating in the original branch of the monolithic transformer but a transversal flux.

C. Uncoupled Inductors and Intercell Transformers

The general properties of intercell transformers being recalled, some of their features can be compared with those of the classical configuration using uncoupled inductors.

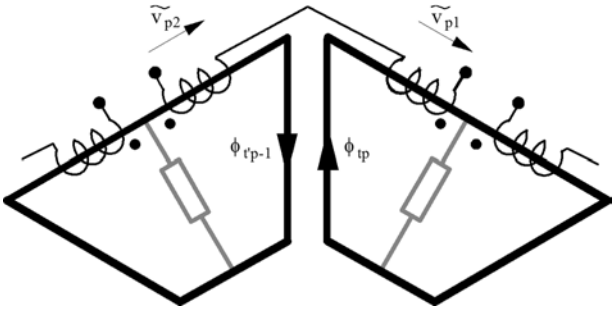

Fig. 7. From the monolithic transformer to the association of transformers.

1) Current Ripples: If Δi_o, is the peak-to-peak output current ripple, the relative ripple in a cell with uncoupled inductors is $k^2 \Delta i_o / I_o$ and is $\Delta i_o / I_o$ with intercell transformers. So, a reasonable relative ripple in a cell (few 10%) with the uncoupled inductors leads to very low values of the relative total ripple with high values of k. That is not necessarily required for the sizing of the output capacitor. For the intercell transformer, the relative ripples are the same for the cell current and for the total output current.

2) Dynamic Response: If the two solutions are designed to obtain the same relative ripple current in a cell, the equivalent output inductor of the intercell transformers is k^2 lower than the one of the other solution. The intercell transformers can thus provide a faster dynamic response.

3) Transformer Behavior: Concerning the winding losses, it is well known that the transformer behavior is better than the inductor one. The magnetic field is unidirectional in the winding window and the eddy current effects can be limited by a appropriate winding layout. This is not true for the inductor, and in addition, the possible air gap generates extra winding losses.

4) Induction Amplitude: The dc current I_o flowing through the magnetic devices creates a dc magnetic field B_o in the core. In the inductor, the ratio $\Delta B_M / B_o$ is identical to the ratio $\Delta i_o / 2 I_o$ (ΔB_M peak value of the ac magnetic field). By contrast, B_o is very small in an intercell transformer with high values of k. The dc field shifting the operating point toward the saturation field, ΔB_M may be higher in the transformer core than in the inductor core, leading to a decrease of the core volume.

For these reasons, it is important to evaluate converters topologies using intercell transformers with a high number of cells. Nevertheless, the previous remarks do not take into account a flux concentration that appears in the transversal branches of the intercell transformer. This phenomenon is described in the next section and a solution to eliminate this drawback is presented in Section IV.

D. Limitations

In case of supply by a regular voltage system, the previous topologies (either monolithic or with separate transformers) leads to oversized magnetic cores. That can be emphasized by considering the alternating transversal flux of the monolithic transformer supplied by a balanced sinusoidal voltage system (in this case, the leakage flux is null because it is the sum of k balanced sinusoidal fluxes). For each main branch

$$\tilde{\phi}_p = \tilde{\phi}_{tp} - \tilde{\phi}_{t'p-1}. \qquad (12)$$

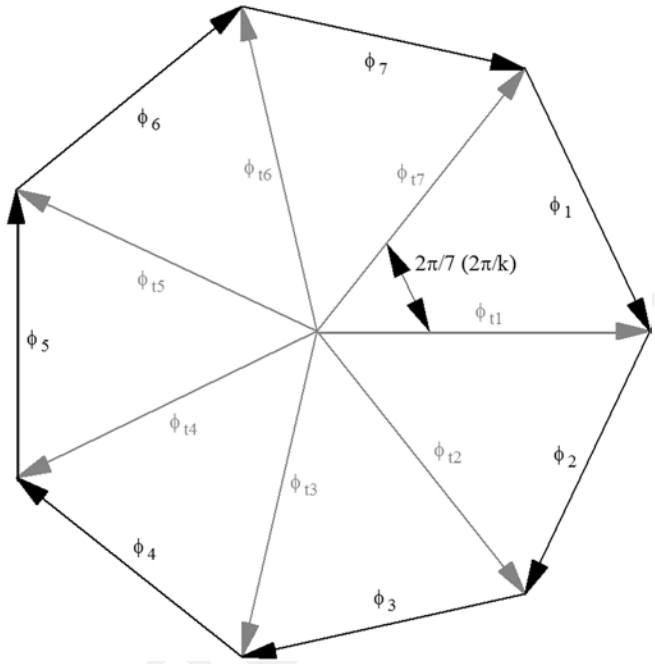

Fig. 8. Diagram of flux vectors for a direct supply system.

TABLE I
INCREASE OF TRANSVERSAL FLUX VERSUS k.

k	2	3	4	5	6	7
$2\lvert\tilde{\phi}_{tp}\rvert / \lvert\tilde{\phi}_p\rvert$	1	1.154	1.414	1.7	2	2.304

The flux $\tilde{\phi}_p$ is imposed by the voltage applied to the corresponding main branch. For a balanced voltage system, the main flux system is also balanced, as the transversal flux system. These properties, associated to (12), lead to the vector diagram of Fig. 8, represented in a particular case ($k = 7$) but that can be generalized to any number of phases.

From this diagram, the relation between the main and transversal fluxes can be easily derived

$$\left|\tilde{\phi}_{tp}\right| = \frac{\left|\tilde{\phi}_p\right|}{2} \frac{1}{\sin\frac{\pi}{k}}.$$

This relation shows the increase of the transversal flux with the number of cells (Table I).

For the monolithic transformer, only the transversal branches have to be oversized. Some monolithic topologies, with main branches connected to a magnetic equipotential, can avoid this problem but the realization become critical. In the separate transformers, the core flux is identical to a tranversal flux of the monolithic transformer and so, the whole core is concerned by the oversizing, with the ratio $2\left|\tilde{\phi}_{tp}\right| / \left|\tilde{\phi}_p\right|$.

At this point, and always in the aim of a high number of cells, this oversizing problem limits the interest of the transformer solution compared to the separate inductors solution. In the next section, a solution based on the modification of the supply system eliminating this major limitation will be presented.

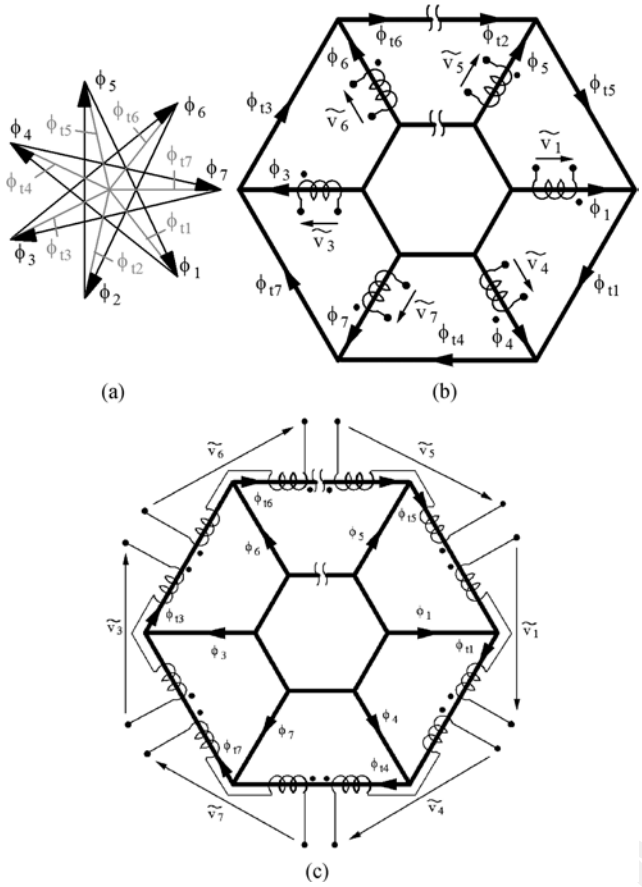

Fig. 9. Modified supply system for reduction of transversal flux. (a) Permutated vector diagram. (b) Permutated supply system. (c) Permutated supply system for separate windings configuration.

IV. Optimization of the Supply Voltage System

A. Principle

The solution to the oversizing identified above is a permutation of the voltage system. Indeed, by modifying the phase sequence, the ratio $2\left|\tilde{\phi}_{tp}\right| / \left|\tilde{\phi}_{p}\right|$.can be reduced and get closer to the ideal value of 1. The vector diagram of Fig. 9(a) illustrates an example of permutation ($k = 7$) leading to a major decrease of the transversal flux.

To obtain this decrease, the main flux has to be composed by two transversal vectors of which phase-shift is not $2\pi/k$ but as close to π as possible ($6\pi/7$ in the current example). Then, the ratio $2\phi_{tp}/\phi_p$ is considerably reduced [from 2.3 in regular mode to 1.025 for permutated mode with $k = 7$)]. To realize this operation, the k windings of the transformer are supplied by a permutated combination of the voltage system generated by the converter cells, as shown on Fig. 9(b). In this example, the right sequence is 1,4,7,3,6,2,5 instead of the regular sequence 1,2,3,4,5,6,7. This principle can be easily generalized to any odd number of cells, with an optimal phase-shift between the transversal flux that is

$$\psi = \frac{(k-1)\pi}{k}.$$

The ratio $2\phi_{tp}/\phi_p$ becomes

$$\left|\tilde{\phi}_{tp}\right| = \frac{\left|\tilde{\phi}_{p}\right|}{2} \frac{1}{\sin\frac{(k-1)\pi}{2k}}.$$

TABLE II
Limitation of the Transversal Flux

k	3	5	7	9	11	13
$2\lvert\tilde{\phi}tp\rvert / \lvert\tilde{\phi}p\rvert$ regular	1.155	1.7	2.3	2.92	3.55	4.18
$2\lvert\tilde{\phi}tp\rvert / \lvert\tilde{\phi}p\rvert$ permutated	1.155	1.05	1.025	1.015	1.01	1.007

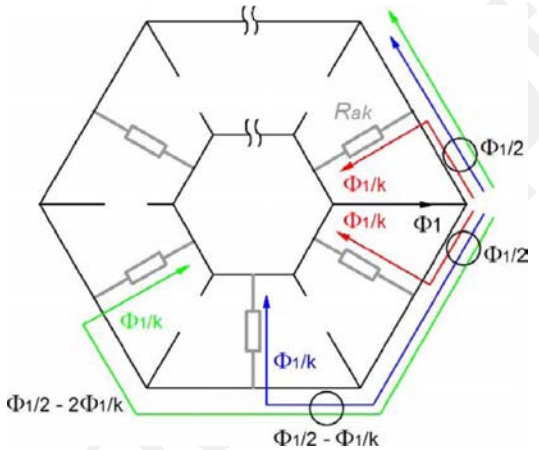

Fig. 10. Repartition of a main flux in the core.

The Table II gives the evolution of the ratio $2\left|\tilde{\phi}_{tp}\right| / \left|\tilde{\phi}_{p}\right|$ in permutated mode compared to the regular mode for odd values of k. The ratio is close to 1 for $k \geq 5$. The oversizing observed with the regular supply system disappears.

The permutated voltage sequence can be also applied to the two-winding configuration, by using the scheme of Fig. 9(c). In that case, the phase-shift between the voltage v'_{p1} and v'_{p2} of two associated windings is $\pi - \psi = \pi/k$, the total vector $v'_{p1} + v'_{p2}$ being equal to v_p. In the same way, the "cyclic cascade" association can be improved by using the supply system of Fig. 9(c).

B. Non-Sinusoidal Supply System

The previous considerations were based on a sinusoidal analysis. It is necessary to verify the interest of the permutated mode in the non-sinusoidal operating mode generated by the converter cells.

In an intercell transformer supplied by k buck cells, the main fluxes is triangular. The shape of the transversal fluxes can be derived from the scheme of Fig. 10 that shows the distribution of one main flux (Φ_1) in the different air branches (with the assumption of transversal reluctances negligible compared to air reluctances, see Section III-A1).

In a symmetrical topology, the distribution is balanced and the flux in each air branches is Φ_1/k. The transversal flux distribution due to one main flux is represented Fig. 10. Then, by superposing the contribution of each main flux, the total flux in any transversal branches can be calculated.

For example, for a seven-cells buck with a regular supply, the expression of a transversal flux is

$$\Phi_{t1} = \frac{1}{2}\Phi_1 + \frac{5}{14}(\Phi_7 - \Phi_2) + \frac{3}{14}(\Phi_6 - \Phi_3) + \frac{1}{14}(\Phi_5 - \Phi_4). \quad (13)$$

The other transversal flux can be deduced by a circular permutation of the index.

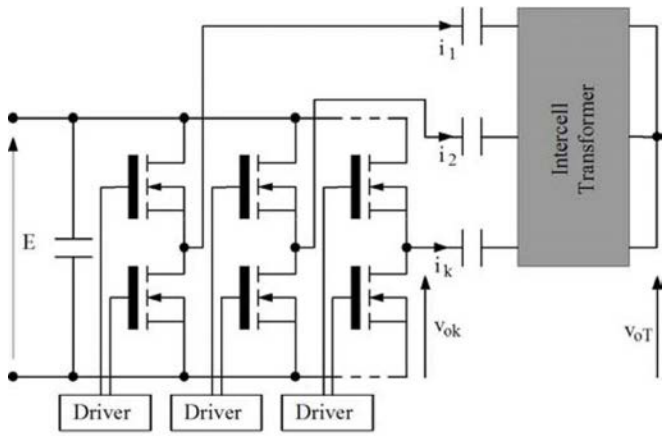

a – Test bench

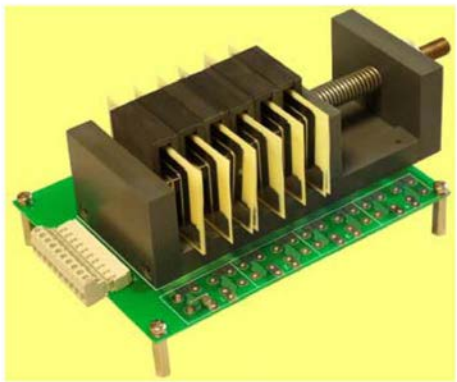

b – Intercell transformer

Fig. 11. Experimental test bench.

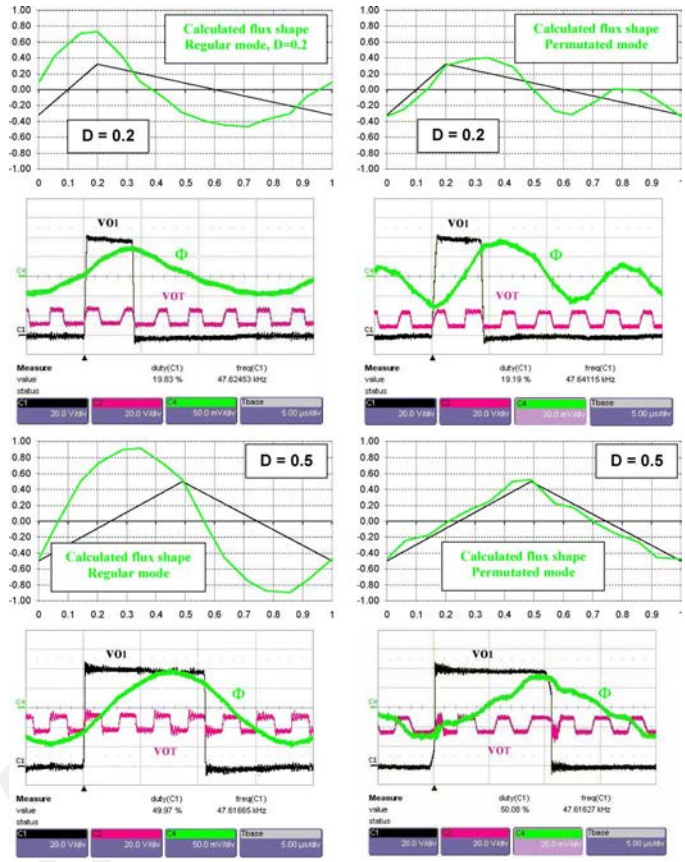

Fig. 12. Calculated and experimental flux shapes.

In case of permutated supply, the expression becomes

$$\Phi_{t1} = \frac{1}{2}\Phi_1 + \frac{5}{14}(\Phi_5 - \Phi_4) + \frac{3}{14}(\Phi_2 - \Phi_7) + \frac{1}{14}(\Phi_6 - \Phi_3). \quad (14)$$

These expressions can also be used for separate transformers in a cyclic-cascade configuration (Fig. 2). In that case, they give directly the shape of the flux flowing through the core of each transformer.

The shapes of the transversal fluxes corresponding to triangular main fluxes can now be reconstituted as shown Fig. 12. The reconstitution results are given for two duty cycles (0.2 and 0.5) and for the two supply modes, regular and permutated. The high decrease of the transversal flux induced by the permutated supply mode can be observed. The triangular shape appearing in the graphs is an ideal (and virtual) one that should exist if the main flux was linearly divided into the two adjacent transversal branches.

C. Experimental Results

To validate this analysis, the test bench of Fig. 11(a) has been realized. It is not designed to deliver power (floating common node) but the voltages applied to the windings are the same as in a seven-cell buck converter and create the same flux waveforms. The intercell transformer is constituted of separate planar transformers [Fig. 11(b)], arranged in cyclic cascade configuration and using 3C90 material. The PCB windings are sized for the magnetizing current only. The series capacitors eliminate the dc voltage components across the windings due to a possible unbalance. The fluxes are measured by placing one turn around the core and by integrating the voltage.

The theoretical and experimental results are compared in Fig. 12 and a very good agreement is obtained It should be noted that the flux scale is 50 mV/div for the regular mode and 20 mV/div for the permutated mode. The very significant reduction of the flux in the second case is confirmed.

In addition, a core losses evaluation has been made with a calorimetric method, based on a preliminary measurement of the calorific capacity of the used cores. The results are summarized Fig. 13.

The reference curve “inductor” corresponds to a configuration providing a triangular flux shape in the core that can be considered as an ideal case, compared to the complex flux shapes created in the intercell transformers. For that, the two windings of the transformers are series-connected and supplied by a cell-voltage, always trough the series capacitor.

The two others curves are derived from measurements made with the cyclic cascade arrangement, in regular and permutated modes. The three curves give the total losses in the seven cores, versus the duty-cycle, with the same dc voltage (100 V) and the same frequency (50 kHz). They are supposed to be symmetrical with respect to the duty cycle 0.5, because the flux shapes are symmetrical. For this reason, the measurements have not made above 0.5.

Once again, the improvement resulting of the permutated mode use is demonstrated, with losses four times lower than

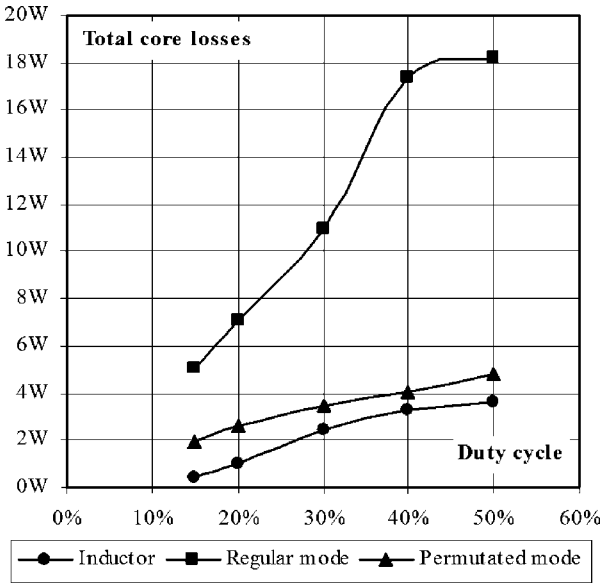

Fig. 13. Core losses in the different configurations.

those generated by the regular mode, for $D = 0.5$. The performances of the permutated cyclic cascade configuration are very close to the ideal triangular case [10]–[14].

V. Conclusion

In this paper, before a recall of topologies and properties of intercell transformers used to achieve the interleaving of electronic converters, a systematic oversizing problem, not clearly described in the literature, is emphasized. It appears in the most widely used configuration where the supplying of intercell transformers by the voltage system is regular. It becomes more critical when the cell number is increased. To solve this problem, a solution has been proposed that consists of an optimal permutation of the voltage sequence, the improvement being as better as the cell number is high. This permutated mode makes the transformer solution very attractive, especially in frequency range where magnetic materials can be used near the saturation field (medium frequency converters). More generally, and with the development of power integration technologies, the design of multi-phase ($k > 5$) interleaved converters using multiphase transformers have to be seriously evaluated.

References

[1] I. G. Park and S. I. Kim, "Modeling and analysis of multi-intercell transformers for connecting power converters in parallel," in *Proc. PESC'97*, 1997, vol. 2, pp. 1164–1170.

[2] T. Meynard and P. Davancens, "Current balance in paralleled commutation cells," in *Proc. Power Conv. Intell. Motion*, Nuremberg, Germany, Jun. 1995.

[3] R. S. Manoj and N. Y. Latham, "Controlled Leakage Field Multi-Intercell Transformer Employing C-Shaped Laminated Magnetic Cores," U.S. Patent 5 379 207, 1995.

[4] P.-L. Wong, P. Xu, B. Yang, and F. C. Lee, "Performance improvements of interleaving VRMs with coupling inductors," in *Proc. APEC'00*, 2000, pp. 973–978.

[5] P. Zumel, O. Garcia, J. A. Cobos, and J. Uceda, "Magnetic integration for interleaved converters," in *Proc. APEC'03*, 2003, vol. 2, pp. 1143–1149.

[6] J. Li, C. R. Sullivan, and A. Schultz, "Coupled inductors design optimization for fast-response low-voltage DC-DC converters," in *Proc. APEC'02*, 2002, vol. 2.

[7] J. Li, A. Stratakos, A. Schultz, and C. R. Sullivan, "Using coupled inductors to enhance transient performance of multi-phase buck converters," in *Proc. APEC'04*, 2004, vol. 2, pp. 1289–1293.

[8] P. Zumel, O. Garcia, J. A. Cobos, and J. Uceda, "Tight magnetic coupling in multiphase interleaved converters based on simple transformers," in *Proc. APEC'05*, 2005, vol. 1, pp. 385–391.

[9] O. Garcia, P. Zumel, A. de Castro, J. A. Cobos, and J. Uceda, "An automotive 16 phases DC-DC converter," in *Proc. PESC'04*, 2004, pp. 350–355.

[10] J. Czogalla, J. Li, and C. R. Sullivan, "Automotive application of multi-phase coupled inductor DC-DC converter," in *Proc. IAS'03*, 2003, vol. 3, pp. 1524–1529.

[11] W. T. Mac Lyman, *Transformers and Inductor Ddesign Handbook*. New York: Marcel Dekker, 1988.

[12] W. G. Odendaal and J. Ferreira, "Effects of scaling high frequency transformers parameters," *IEEE Trans. Ind. Appl.*, vol. 35, no. 4, pp. 932–940, Jul./Aug. 1999.

[13] W. G. Odendaal and J. Ferreira, "A thermal model for high-frequency magnetic components," *IEEE Trans. Ind. Appl.*, vol. 35, no. 4, pp. 924–931, Jul./Aug. 1999.

[14] H. Njiende, N. Fröhleke, and J. Böcker, "Optimized size design of integrated magnetic component using area product approach," in *Proc. EPE Conf.*, Dresden, Germany, 2005, p. 10.